

The circular-polarization phase-meter

Boris Bergues*

Laboratory for Attosecond Physics, Max-Planck-Institut für Quantenoptik,
Hans-Kopfermann-Strasse 1, D-85748 Garching, Germany

[*boris.bergues@mpq.mpg.de](mailto:boris.bergues@mpq.mpg.de)

Abstract: A new method to measure the carrier-envelope phase (CEP) of a strong few-cycle laser pulse is introduced. The new concept relies on above threshold ionization (ATI) in circularly polarized laser fields and allows for CEP tagging every single laser pulse generated in few-cycle laser systems at multi-kHz repetition rates. The implementation of the new method is described and discussed quantitatively. It is shown that the introduced circular-polarization phase-meter may offer a series of advantages over existing CEP-tagging schemes based on ATI in linearly polarized laser fields.

© 2012 Optical Society of America

OCIS codes: (320.7160) Ultrafast technology; (320.7100) Ultrafast measurements; (320.2250) Femtosecond phenomena; (020.2649) Strong field laser physics; (020.4180) Multiphoton processes.

References and links

1. M. Nisoli, S. De Silvestri, O. Svelto, R. Szipöcs, K. Ferencz, Ch. Spielmann, S. Sartania, and F. Krausz, "Compression of high-energy laser pulses below 5fs," *Opt. Lett.* **22**, 522–524 (1997).
2. X. Gu, G. Marcus, Y. Deng, T. Metzger, C. Teisset, N. Ishii, T. Fuji, A. Baltuska, R. Butkus, V. Pervak, H. Ishizuki, T. Taira, T. Kobayashi, R. Kienberger, and F. Krausz, "Generation of carrier-envelope-phase-stable 2-cycle 740-J pulses at 2.1-m carrier wavelength," *Opt. Express* **17**(1), 62–69 (2009).
3. M. Hentschel, R. Kienberger, Ch. Spielmann, G. A. Reider, N. Milošević, T. Brabec, P. Corkum, U. Heinzmann, M. Drescher, and F. Krausz, "Attosecond metrology," *Nature* **414**, 509–513 (2001).
4. F. Krausz, and M. Ivanov, "Attosecond physics," *Rev. Mod. Phys.* **81**, 163–234 (2009).
5. A. Baltuška, T. Fuji, and T. Kobayashi, "Controlling the Carrier-envelope phase of ultrashort light pulses with optical parametric amplifiers," *Phys. Rev. Lett.* **88**, 133901 (2002)
6. B. Bergues, S. Zharebtsov, Y. Deng, X. Gu, I. Znakovskaya, R. Kienberger, F. Krausz, G. Marcus, and M. F. Kling, "Sub-cycle electron control in the photoionization of xenon using a few-cycle laser pulse in the mid-infrared," *New J. Phys.* **13**, 063010 (2011).
7. J. Reichert, R. Holzwarth, Th. Udem, and T. W. Hansch, "Measuring the Frequency of Light with Mode-locked Lasers," *Opt. Commun.* **172**, 59–68 (1999).
8. H. R. Telle, G. Steinmeyer, A. E. Dunlop, J. Stenger, D. H. Sutter, and U. Keller, "Carrier-envelope offset phase control: A novel concept for absolute optical frequency measurement and ultrashort pulse generation," *Appl. Phys. B* **69**, 327–332 (1999).
9. D. J. Jones, S. A. Diddams, J. K. Ranka, Andrew Stentz, Robert S. Windeler, John L. Hall, and Steven T. Cundiff, "Carrier-envelope phase control of femtosecond mode-locked lasers and direct optical frequency synthesis," *Science* **288**, 635–639 (2000).
10. A. Apolonski, A. Poppe, G. Tempea, Ch. Spielmann, Th. Udem, R. Holzwarth, T. W. Hänsch, and F. Krausz, "Controlling the phase evolution of few-cycle light pulses," *Phys. Rev. Lett.* **85**, 740–743 (2000).
11. T. Udem, R. Holzwarth, and T. W. Hänsch, "Optical frequency metrology," *Nature* **416**, 233–237 (2002).
12. S. T. Cundiff, "Phase stabilization of ultrashort optical pulses," *J. Phys. D* **35**, R43–R59 (2002).
13. A. Baltuška, Th. Udem, M. Uiberacker, M. Hentschel, E. Goulielmakis, Ch. Gohle, R. Holzwarth, V. S. Yakovlev, A. Scrinzi, T. W. Hänsch, and F. Krausz, "Attosecond control of electronic processes by intense light fields," *Nature* **421**, 611–615 (2003).
14. P. Agostini, F. Fabre, G. Mainfray, G. Petite, and N. K. Rahman, "Free-free transitions following six-photon ionization of xenon atoms," *Phys. Rev. Lett.* **42**, 1127–1130 (1979).

15. G. G. Paulus, F. Grasbon, H. Walther, P. Villoresi, M. Nisoli, S. Stagira, E. Priori, and S. De Silvestri, "Absolute-phase phenomena in photoionization with few-cycle laser pulses," *Nature* **414**, 182–184 (2001).
16. P. Dietrich, F. Krausz, and P. B. Corkum, "Determining the absolute carrier phase of a few-cycle laser pulse," *Opt. Lett.* **25**, 16–18 (2000).
17. G. G. Paulus, F. Lindner, H. Walther, A. Baltuka, E. Goulielmakis, M. Lezius, and F. Krausz, "Measurement of the phase of few-cycle laser pulses," *Phys. Rev. Lett.* **91**, 253004 (2003).
18. T. Wittmann, B. Horvath, W. Helml, M. G. Schätzel, X. Gu, A. L. Cavalieri, G. G. Paulus, and R. Kienberger, "Single-shot carrier-envelope phase measurement of few-cycle laser pulses," *Nature Phys.* **5**, 357–362 (2009).
19. Zhangjin Chen, T. Wittmann, B. Horvath, and C. D. Lin, "Complete real-time temporal waveform characterization of single-shot few-cycle laser pulses," *Phys. Rev. A* **80**, 061402(R) (2009).
20. F. Süßmann, S. Zharebtsov, J. Plenge, Nora G. Johnson, M. Kübel, A. M. Sayler, V. Mondes, C. Graf, E. Rühl, G. G. Paulus, D. Schmiscke, P. Swrschek, and M. F. Kling, "Single-shot velocity-map imaging of attosecond light-field control at kilohertz rate," *Rev. Sci. Instrum.* **82**, 093109 (2011).
21. N. G. Johnson, O. Herrwerth, A. Wirth, S. De, I. Ben-Itzhak, M. Lezius, B. Bergues, M. F. Kling, A. Senftleben, C. D. Schröter, R. Moshhammer, J. Ullrich, K. J. Betsch, R. R. Jones, A. M. Sayler, T. Rathje, K. Rühle, W. Müller, and G. G. Paulus, "Single-shot carrier-envelope-phase-tagged ion-momentum imaging of nonsequential double ionization of argon in intense 4-fs laser fields," *Phys. Rev. A* **83**, 013412 (2011).
22. N. Camus, B. Fischer, M. Kremer, V. Sharma, A. Rudenko, B. Bergues, M. Kübel, N. G. Johnson, M. F. Kling, T. Pfeifer, J. Ullrich, and R. Moshhammer, "Attosecond correlated dynamics of two electrons passing through a transition state," *Phys. Rev. Lett.* **108**, 073003 (2012).
23. B. Bergues, M. Kübel, N. G. Johnson, B. Fischer, N. Camus, K. J. Betsch, O. Herrwerth, A. Senftleben, A. M. Sayler, T. Rathje, T. Pfeifer, I. Ben-Itzhak, R. R. Jones, G. G. Paulus, F. Krausz, R. Moshhammer, J. Ullrich, and M. F. Kling, "Attosecond tracing of correlated electron-emission in non-sequential double ionization," *Nature Commun.* **3**, 813 (2012).
24. G. G. Paulus, "A Meter of the Absolute Phase of Few-Cycle Laser Pulses," *Laser Physics*, **15**, 843–854 (2005).
25. T. Rathje, N. G. Johnson, M. Möller, F. Süßmann, D. Adolph, M. Kübel, R. Kienberger, M. F. Kling, G. G. Paulus, and A. M. Sayler, "Review of attosecond resolved measurement and control via carrier-envelope phase tagging with above-threshold ionization," *J. Phys. B* **45**, 074003 (2012).
26. A. M. Sayler, Tim Rathje, Walter Müller, Klaus Rühle, R. Kienberger, and G. G. Paulus, "Precise, real-time, every-single-shot, carrier-envelope phase measurement of ultrashort laser pulses," *Opt. Lett.* **36**, 1–3 (2011).
27. For a review on rescattering in ATI see for instance: W. Becker, F. Grasbon, R. Kopold, D. B. Milošević, G. G. Paulus, and H. Walther, "Above-threshold ionization: From classical features to quantum effects," *Adv. At. Mol. Opt. Phys.* **48**, 35–98 (2002).
28. M. F. Kling, J. Rauschenberger, A. J. Verhoef, E. Hasović, T. Uphues, D. B. Milošević, H. G. Muller, and M. J. J. Vrakking, "Imaging of carrier-envelope phase effects in above-threshold ionization with intense few-cycle laser fields," *New J. Phys.* **10**, 025024 (2008).
29. B. Bergues, Y. F. Ni, H. Helm, and I. Yu. Kiyani, "Experimental study of photodetachment in a strong laser field of circular polarization," *Phys. Rev. Lett.* **95**, 263002 (2005).
30. Boris Bergues, Zunaira Ansari, Dag Hanstorp, and Igor Yu. Kiyani, "Photodetachment in a strong laser field: An experimental test of Keldysh-like theories," *Phys. Rev. A* **75**, 063415 (2007).
31. A. Gazibegović-Busuladžić, D. B. Milošević, W. Becker, B. Bergues, H. Hultgren, and I. Yu. Kiyani, "Electron rescattering in above-threshold photodetachment of negative ions," *Phys. Rev. Lett.* **104**, 114102 (2010).
32. M. Kübel, K. J. Betsch, Nora G. Johnson, U. Kleineberg, R. Moshhammer, J. Ullrich, G. G. Paulus, M. F. Kling, and B. Bergues, "Carrier-envelope-phase tagging in measurements with long acquisition times," *New J. Phys.* **14**, 093027 (2012).
33. X. M. Tong, and C. D. Lin, "Empirical formula for static field ionization rates of atoms and molecules by lasers in the barrier-suppression regime," *J. Phys. B*, **38**, 2593–2600 (2005).
34. A. Apolonski, P. Dombi, G. G. Paulus, M. Kakehata, R. Holzwarth, Th. Udem, Ch. Lemell, K. Torizuka, J. Burgdörfer, T. W. Hänsch, and F. Krausz, "Observation of light-phase-sensitive photoemission from a metal," *Phys. Rev. Lett.* **92**, 073902 (2004).

1. Introduction

The development of laser sources producing strong near single-cycle pulses in the near-infrared [1] and infrared [2] has led to great advances in strong field physics. In particular, it has allowed for resolving electron dynamics on sub-femtosecond time scales [3], thus marking the advent of time-domain attosecond physics [4]. The electric field of a short laser pulse

propagating in z-direction can be described as

$$\mathbf{E}(t) = \frac{E_0 \cos^2(\pi t/\tau)}{\sqrt{1 + \varepsilon^2}} [\cos(\omega t + \phi), \varepsilon \sin(\omega t + \phi), 0], \quad (1)$$

where E_0 is the field amplitude, ε the ellipticity, ω the carrier frequency, τ the pulse duration, and ϕ the CEP. In the few- to single-cycle regime, the value of the CEP strongly affects the temporal shape of the electric field and the knowledge of the CEP becomes essential to fully characterize the laser pulse.

Apart from intrinsically CEP-stable optical parametric chirped-pulse amplification systems in the infrared [2, 5], for which the CEP was demonstrated to remain stable over many hours without the need of any active stabilization [6], the generation of strong CEP-stable few-cycle pulses relies on CEP stabilization of the seed pulses [7–12]. The CEP of the amplified CEP-stable seed pulses undergoes slow drifts that can be eliminated with an additional slow feedback loop [13]. Active CEP stabilization of the seed pulses, however, introduces instabilities in the oscillator, which limits stable operation to a few hours and hampers CEP-resolved measurements of low count-rate processes. A solution to this problem is to measure the CEP instead of stabilizing it. If the amplifier is seeded with non-phase stabilized pulses, however, the CEP of the amplified pulses is randomly distributed and has to be determined for every single laser shot.

The idea of using ATI [14] of noble gas atoms in linearly or circularly polarized laser fields to perform CEP measurements was proposed a decade ago in Refs [15] and [16] respectively. The measurement of the CEP using ATI in linearly polarized laser fields has been realized with the “stereo-ATI phase-meter” [17]. Further developments of this technique have finally lead to the “single-shot stereo-ATI phase-meter” [18], which allows for single-shot CEP measurements and even waveform characterization [19] at multi-kHz repetition rates. The new CEP-tagging technique has been combined with single-shot electron imaging spectroscopy [20] as well as electron-ion coincidence spectroscopy [21] and has recently allowed for tracing the correlated electron emission in non-sequential double ionization on attosecond time scales, using few-cycle [22] and near-single cycle [23] laser pulses.

The principle of single-shot CEP measurements via ATI of xenon in linearly polarized laser pulses has been described in detail in the literature (see for instance Refs. [24, 25]). It is based on the CEP dependence of the asymmetry $A = (N_+ - N_-)/(N_+ + N_-)$ in the yields N_+ and N_- of ATI electrons emitted with opposite momentum. The CEP-dependent asymmetry $A(\phi)$ is a periodic function of the CEP with period 2π . In the first approximation it has the form $A(\phi) = a \cos(\phi + \phi_0)$, where a is the asymmetry amplitude, ϕ the CEP and ϕ_0 an unknown but constant CEP offset value. Because $A(\phi)$ is not a bijective function, the CEP cannot be determined unambiguously from the measurements of a single asymmetry $A(\phi)$. An unambiguous determination of the CEP is possible, though, if two phase shifted CEP-dependent asymmetries $A_x(\phi) = a_x \cos(\phi + \phi_{0x})$ and $A_y(\phi) = a_y \cos(\phi + \phi_{0y})$ can be measured simultaneously for each laser pulse. Plotting A_y versus A_x results in a parametric asymmetry plot (PAP) [18]. The one to one relation between the CEP ϕ and the polar angle θ parametrizing the PAP can easily be determined from the knowledge that the CEP of a non-phase-stabilized amplified laser pulse is uniformly randomly distributed [26]. In the stereo-ATI phase-meter, the two phase shifted asymmetries A_x and A_y are measured in two separate regions of the high-energy part of the electron’s kinetic-energy spectrum, i.e. in the so called rescattering plateau [27]. In this part of the spectrum, where the asymmetry is the most pronounced [28], the CEP offset ϕ_0 in $A(\phi)$ is increasing with the kinetic energy of the electron, providing the required phase shift between the two CEP-dependent asymmetries.

In contrast to the stereo-ATI phase-meter, the proposed circular-polarization phase-meter (CPP-meter) does not rely on the rescattering process. Instead, it takes advantage of the CEP-

depend emission-direction of electrons ionized in circularly polarized laser pulses. While it makes a more efficient use of the ionization signal, the CPP-meter also eliminates the need for electron TOF-spectra measurements, which should make it a robust, easy to implement and user-friendly device.

2. Principle and implementation of a circular-polarization phase-meter

In ATI with linearly polarized laser pulses, most electrons are emitted in the vicinity of a cycle maximum or minimum. Electrons ionized just before and just after the cycle maximum or minimum are emitted in opposite directions along the laser polarization axis. Since the intensity envelope of the pulse changes only minimally across a single maximum or minimum of the field, the left-right asymmetry in the yields is very small. The trick employed in the stereo-ATI phase-meter is to restrict the yield measurement to the high-energy region of the photo-electron spectrum. In this region that constitutes the rescattering plateau, only electrons emitted just after the maximum (or minimum) of a laser cycle contribute to the yield. Electrons emitted with opposite momenta in the rescattering plateau were thus ionized in different half cycles. Since the intensity envelope of a few cycle pulse undergoes significant changes within half a laser period, the left-right asymmetry in the yield of electrons is dramatically enhanced in the rescattering plateau. While the build-up of the rescattering plateau requires rather high laser intensities, the 'useful' rescattered electron signal represents, however, only a tiny fraction of the total ionization yield.

The new scheme makes use of circular polarization to obtain similar high asymmetry amplitudes as in the stereo-ATI phase-meter, but without the need to restrict the measurement to a small fraction of the ionization yield. Electrons ionized in a strong circularly polarized laser field are preferentially emitted in the polarization plane. In strong field approximation (SFA), i.e. when the interaction of the electron with its parent core is neglected after ionization, the final electron momentum is perpendicular to the direction of the electric field at the moment of ionization (SFA was shown to work very reliably for systems with a short-range binding potential [29–31]). Electrons emitted in opposite (\pm) directions therefore originate from different half cycles. As in the case of rescattered electrons, this leads to high asymmetries in the corresponding yields Y_{\pm} . It can be seen from Eq. (1), that the CEP of a circularly polarized laser pulse coincides with the angle of the electric field vector when the latter reaches its maximum absolute value at $t = 0$. In cases where SFA is valid and depletion of the target population is negligible, the direction θ of maximum asymmetry in the yields Y_{\pm} of ATI electrons is thus $\theta = \phi - \pi/2$. In this case, the absolute CEP is simply obtained by measuring the direction of maximum asymmetry. In general, however, the electron-core interaction as well as depletion effects can induce an additional CEP-independent shift θ_0 of the emission angle. Unless extra theoretical input is provided, the value of this shift is unknown, so that the measured CEPs are only determined up to a constant offset phase.

A design for a CPP-meter is proposed in Fig. 1. Similar to the stereo-ATI phase-meter, near-infrared few-cycle laser pulses (propagating along the z-axis of the coordinate system in Fig. 1) are focused into a gas cell at the origin of the coordinate system, where electrons are generated via strong field ionization of xenon atoms. Electrons leaving the gas cell through small openings are recorded by detectors placed in front of those openings. While in the stereo-ATI phase-meter electrons are detected on opposite sides of the gas cell along the x-direction, in the CPP-meter, two additional openings and electron detectors are added on either side of the gas cell along the y-axis. For each circularly polarized input pulse, four numbers, i.e. the yields $N_{\pm x}$ and $N_{\pm y}$ of electrons emitted in $\pm x$ and $\pm y$ directions, respectively, are recorded by the four detectors. The two CEP dependent asymmetries A_x and A_y in the yield of electrons emitted in $\pm x$ and $\pm y$ directions are calculated as $A_x = (N_{+x} - N_{-x}) / (N_{+x} + N_{-x})$ and $A_y = (N_{+y} - N_{-y}) / (N_{+y} + N_{-y})$,

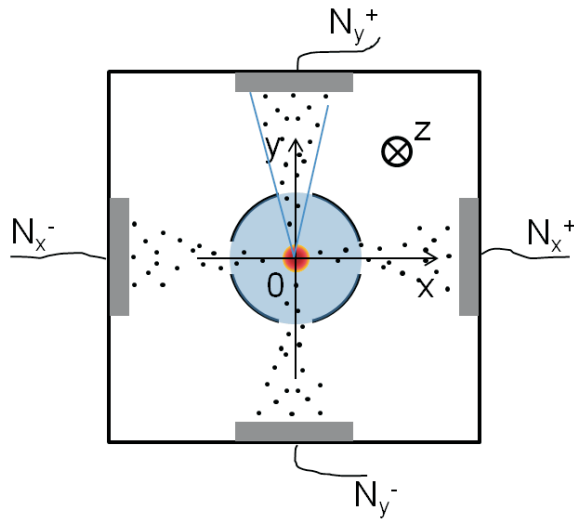


Fig. 1. Sketch of a circular-polarization phase-meter. Few-cycle circularly polarized laser pulses (propagating along the z -axis) are focused into a cell (black circle) containing xenon gas (blue on the picture) and located in the center of a vacuum chamber (surrounding black square). Electrons (small black dots) generated in the laser focus (red disk) leave the gas cell through small openings situated on the left, right, top, and bottom of the cell and are registered by detectors (gray) placed in front of the openings. The measured electron yields N_{+x} , N_{-x} , N_{+y} , and N_{-y} are used to calculate the two asymmetries A_x and A_y .

respectively.

A direct advantage of the CPP-meter over the stereo-ATI phase-meter is that there is no need to record the electron's TOF anymore. This allows for a much simpler detection scheme, which does not require fast up-stream electronics since only four numbers i.e. the yields N_{+x} , N_{-x} , N_{+y} and N_{-y} have to be measured for each laser shot. Another advantage of the new method is that the phase shift $\alpha = \phi_{0y} - \phi_{0x}$ between the measured asymmetries A_x and A_y is only determined by the geometry of the apparatus. For the arrangement shown in Fig. 1, $\alpha = 90^\circ$ and the PAP will thus have a nearly circular shape, independently of the laser intensity. This is in contrast to the stereo-ATI phase-meter, where the fact that α depends on several parameters (e.g. the particular regions considered in the rescattering plateau or the input pulse energy) [32] complicates somewhat the comparison of PAPs recorded under different experimental conditions.

3. Simulation of CPP-meter measurements

In order to demonstrate the feasibility of the new method, a CPP-meter measurement is simulated for realistic parameters. The laser pulses are described using Eq. (1). Circularly polarized pulses ($\varepsilon = 1$), with a duration of 4 fs (in the following, pulse durations refer to the FWHM of the intensity envelope) and a pulse energy of 12 μJ are calculated for 24 different CEP values $\phi = 15^\circ, 30^\circ, \dots, 360^\circ$. The pulses are focused to a waist of 80 μm FWHM into the gas cell filled with 10^{-3} mbar of xenon. The peak E_0 of the electric field amounts to 3.27×10^{-2} a.u., which corresponds to an intensity $E_0^2 = 3.73 \times 10^{13}$ W/cm². The time dependent tunnel ionization rate of a xenon atom during the interaction with the laser pulse is calculated using the static field ionization rate of Tong and Lin [33]. Target depletion and focal volume averaging are taken into account in the calculations. Since the size of the openings in the gas cell is small compared to

the Rayleigh range, the intensity variation along the propagation direction was neglected. After tunnel ionization the electrons are propagated as classical particles in the electric field of the laser and the Coulomb potential of the parent core. The trajectories are started at the exit of the tunnel with an initial velocity of zero. For each CEP, the expectation values for the number of detected electrons $\bar{N}_{\pm x}$, $\bar{N}_{\pm y}$ are obtained from the calculated yields of electrons emitted in a cone with an apex angle of 30 degree. The detection efficiency is accounted for by multiplying the yields with a factor 0.5. In order to mimic the effect of statistical fluctuations, 100 yields $N_{\pm x}$, $N_{\pm y}$ are generated for each CEP from four Poisson distributions with expectation values $\bar{N}_{\pm x}$ and $\bar{N}_{\pm y}$.

The simulated PAP and the corresponding CEP-resolved momentum distribution of ATI-electrons, projected along the x -axis are shown in Figs. 2(a) and 2(b), respectively. In Fig. 2(a), the blue points are obtained by calculating the asymmetries A_x and A_y using the Poisson distrib-

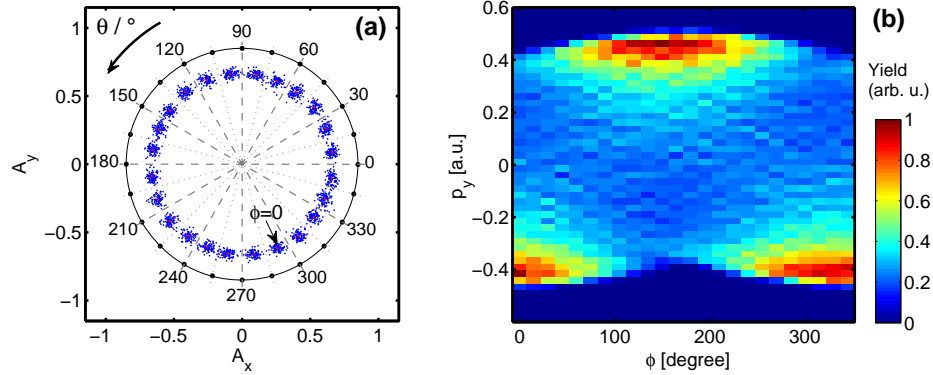


Fig. 2. (a) Simulated PAP obtained for circularly polarized 4-fs laser pulses with CEP values $\phi=0^\circ, 15^\circ, 30^\circ, \dots, 345^\circ$. A pulse energy of $12 \mu\text{J}$ and a xenon gas pressure of 10^{-3} mbar were assumed. The blue points are obtained by calculating the asymmetries A_x and A_y using the Poisson distributed random numbers $N_{\pm x}$, $N_{\pm y}$. The red points are obtained from the expectation values $\bar{N}_{\pm x}$, $\bar{N}_{\pm y}$ (see text for details). The absolute CEP ϕ is related to the polar angle θ of the PAP via $\phi = \theta + \pi/2 - \theta_0$, with $\theta_0 = 23^\circ$. The PAP entry corresponding to $\phi = 0$ is indicated with an arrow. (b) Calculated CEP-resolved momentum distribution of ATI-electrons, projected along the x -axis. The parameters are the same as in (a).

uted random numbers $N_{\pm x}$, $N_{\pm y}$. The red points are obtained from the expectation values $\bar{N}_{\pm x}$, $\bar{N}_{\pm y}$. For the xenon gas pressure of 10^{-3} mbar assumed in the simulation, the statistical error $\Delta\phi$ amounts to 2 degree. For a PAP with nearly circular shape, as in the present case, the statistical error of the CEP can be determined experimentally from the measured radius R and width ΔR of the PAP as $\Delta\phi = 2\pi \Delta R/R$ [26]. For the parameters used in the calculation, the absolute CEP ϕ is related to the polar angle θ of the PAP via $\phi = \theta + \pi/2 - \theta_0$, with $\theta_0 = 22.6^\circ$. Deviations with respect to the above relation, i.e. systematic errors of the relative CEP are found to be smaller than 1.6° . It was verified that a change of 4 percent in the pulse-energy shifts the angle θ by less than 0.5° . It should be noted that in spite of those relatively small systematic errors, the measurement of accurate CEP-dependent ionization-yields requires the application of the renormalization procedure described in Ref. [26] to determine the exact relation $\phi(\theta)$. The reason is that even small deviations of the asymmetry curves $A_x(\phi)$ and $A_y(\phi)$ from sine and cosine functions can significantly affect the measurement of CEP-dependent ionization yields [32]. Additional errors induced by slow drifts of the laser intensity can be reduced to a large extend by a frequent update of the renormalization procedure in the course of the measurement [32].

Repeating the simulation for longer pulses (the peak intensity being kept fixed) shows that while the shape of the PAP remains close to circular, the PAP radius decreases from 0.65 (for pulse durations of 4 fs) to 0.35 and 0.15 for pulse durations of 5 and 6 fs, respectively. For a fixed xenon pressure in the gas cell, the statistical error in the CEP determination increases from 2° (for 4 fs) to 5° and 11° for pulse durations of 5 and 6 fs, respectively.

The robustness of the method with respect to small deviations from perfect circular polarization was tested by repeating the calculations of Fig. 2 for an ellipticity $\varepsilon = 0.93$. While the PAP becomes slightly elliptical (with a ratio of major to minor axis of 1.05), such a 7 percent variation in ε does not significantly affect the results: the statistical errors remain essentially unchanged while the systematic error slightly increases to 1.9° .

In order to investigate the dependence of the CEP measurement on the pulse energy, the calculation of Fig. 2 was repeated for 9 equidistant values of $E_0^2 = 1.5 \times 10^{13} \text{ W/cm}^2, \dots, 7.3 \times 10^{13} \text{ W/cm}^2$. The result of the calculation is presented in Fig. 3(a), where points corresponding

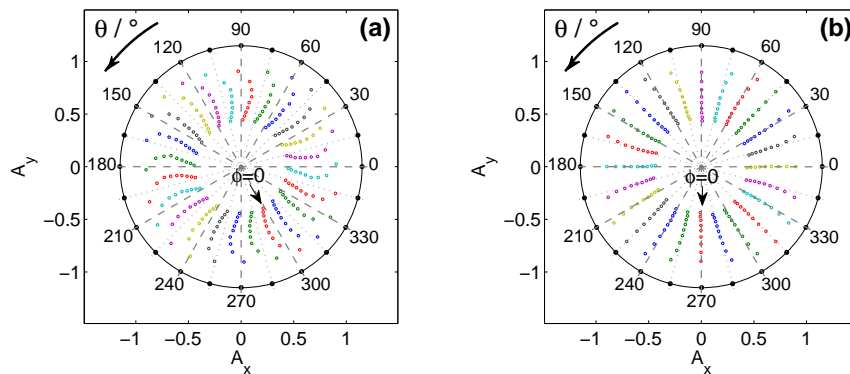


Fig. 3. (a) PAP's calculated for different equidistant intensities ranging from $1.5 \times 10^{13} \text{ W/cm}^2$ to $7.3 \times 10^{13} \text{ W/cm}^2$. All other simulation parameters are the same as in Fig. 2. Points calculated for the same CEP are plotted using the same color. The asymmetry, i.e. the PAP radius decreases with increasing intensity. The PAP entry corresponding to $\phi = 0$ is indicated by an arrow. (b) Same as in (a) but ignoring the Coulomb interaction between the ionized electron and the parent core.

to the same CEP are plotted using the same color for better readability. It can be seen that the asymmetry and thus the radius R of the PAP decrease with increasing intensity, and that the value of the angle θ_0 is also intensity dependent. The reason for the shift θ_0 is the Coulomb interaction. This is demonstrated in Fig. 3(b), where the same calculation was repeated using SFA. For the range of intensities considered here, $\theta_0 = 0$ holds independently of the intensity. It should be noted, however, that this is not true anymore at higher intensities where target depletion becomes significant. In that case the maximum of the ionization yield is reached before the maximum of the laser pulse, which results in a finite shift θ_0 , even in the absence of electron-core interaction after ionization. Nevertheless, the calculations indicate that under conditions where depletion is negligible and SFA is a valid approximation, the absolute CEP could be inferred directly from the measured PAP angle θ .

4. Conclusion

In conclusion, a new way of performing single-shot CEP-measurements using ATI has been introduced and discussed quantitatively. Simulations indicate that the new approach, which relies

on the use of circularly polarized laser pulses, may offer a number of advantages over the existing schemes that use linearly polarized pulses. One of the main assets of the proposed circular-polarization phase-meter is that it eliminates the need for electron TOF-spectra measurements, which should greatly simplify its implementation. In contrast to existing techniques, the electron signal in the CPP-meter is not restricted to a small fraction of the total ionization yield. The 10 to 100 fold higher efficiency in the use of the ionization signal may help to substantially reduce the statistical uncertainty of the CEP measurement. Since the CPP-meter doesn't rely on the rescattering effect, the required input intensity is essentially determined by the ionization potential of the target gas. The choice of a different, for instance metallic, target [34], with a lower ionization potential could allow for adapting the method to much lower input intensities and possibly lead to applications in CEP measurements of non-amplified oscillator pulses.

Acknowledgments

I'm grateful for support from Matthias Kling, Laszlo Veisz, and Ferenc Krausz and greatly appreciated many fruitful discussions with Matthias Kübel, Sergey Zherebtsov, and Harmut Schröder. This work was supported by the Deutsche Forschungsgemeinschaft (DFG), Grant No. KL-1439/3.